

REMARKS

This amendment responds to the office action mailed on February 19, 2003. In the office action the Examiner:

- rejected claims 1, 3-5, 28, 29, 33, 34, 54, 56, 58, and 60-65 under 35 U.S.C. § 103(a) as being unpatentable over Tinkham in view of Char *et al.* (USP 5,157,466);
- rejected claims 2, 30, and 31 under 35 U.S.C. § 103(a) as being unpatentable over Tinkham in view of Char *et al.* and further in view of Shnirman *et al.* (Physical Review B 57, p. 15400, 1998);
- rejected claims 6, 8-10, 35, 39, 40, 41, 53, 55, 57, and 59 under 35 U.S.C. § 103(a) as being unpatentable over Tinkham in view of Char *et al.* and further in view of Baechtold *et al.* (USP 3,953,749);
- rejected claims 7, 11-18, 36, 37, 42, 43, 45, 46, and 48-50 under 35 U.S.C. § 103(a) as being unpatentable over Tinkham in view of Char *et al.*, Baechtold *et al.* and further in view of Shnirman *et al.*; and
- rejected claims 1-18 and 28-65 under the judicially created doctrine of obviousness-type double patenting as being unpatentable over claims 1-6, 12, 14, 15, and 18-25 of U.S. Patent No. 6,459,097 in view of Char *et al.*

After entry of this amendment, the pending claims are claims 1-18 and 28-65. Applicant has amended claims 3 and 65 to correct for antecedent basis. No new matter has been added.

CLAIM REJECTION UNDER 35 U.S.C. § 103(A)

Legal standard

When rejecting claims under 35 U.S.C. § 103, the PTO bears the burden of establishing a *prima facie* case of obviousness. *In re Bell*, 26 USPQ2d 1529 (Fed. Cir. 1993). To establish a *prima facie* case, the prior art reference, or references when combined, must teach or suggest each and every limitation of the claimed invention. MPEP § 706.02(j). The teaching or suggestion to make the claimed invention and the reasonable expectation of success must both be found in the prior art, not in the Applicant's disclosure. *In re Vaeck*, 20 USPQ2d 1438 (Fed. Cir. 1991). There must be some motivation, suggestion, or teaching of the desirability of making the specific

combination that was made by the Applicant. *In re Fine*, 837 F.2d 1071, 1075 (Fed. Cir. 1988).

In the present instance, one relevant inquiry is whether the cited art, either alone or in combination, teaches each and every limitation of the rejected claims. Another relevant inquiry is whether the prior art provides one of ordinary skill in the art with a suggestion or motivation to modify or combine the teachings of the references relied upon by the PTO to arrive at the claimed invention. As discussed in detail below, the cited art fails to satisfy either of these requirements. Therefore, the 35 U.S.C. § 103 rejections should be withdrawn.

Claims 1, 3-5, 28, 29, 33, 34, 54, 56, 58 and 60-65

The PTO has rejected claims 1, 3-5, 28, 29, 33, 34, 54, 56, 58 and 60-65 under 35 U.S.C. 103(a) as being unpatentable over Tinkham in view of Char *et al.* (USP 5,157,466). Applicant respectfully traverses the rejection.

One limitation found in each independent claim in the present application is a clean Josephson junction having unconventional superconducting material on at least one side of the junction, hereinafter referred to as an unconventional superconductor clean Josephson junction. In the December 3, 2002 response to the September 3, 2002 Office Action, the Applicant argued that the bi-epitaxial Josephson junctions described in Char *et al.* are not unconventional superconductor clean Josephson junctions as recited in the claimed invention. In the February 19, 2003 Office Action, the PTO dismissed the unconventional superconductor clean Josephson junction limitation in the independent claims by stating that it would have been obvious to provide the best quality crystal structures since this is standard in semiconductor processing.

Here, the Applicant will describe the current-phase relationship of Josephson junctions made from conventional superconducting materials and unconventional superconducting materials. Then, the current-phase relationship of clean Josephson junctions will be reviewed. Next, the Applicant will discuss why Char *et al.* and Tinkham do not teach or suggest an unconventional superconductor clean Josephson junction and why there is no motivation to modify Char *et al.* to incorporate clean Josephson junctions into Char *et al.* devices.

Josephson junction current-phase relationships

In general, the current-phase relation of a Josephson junction is described by an odd periodic function commonly represented by the Fourier expansion:

$$I(\varphi) = I_1 \cdot \sin(\varphi) + I_2 \cdot \sin(2\varphi) + \dots \quad (1)$$

where I_1 and I_2 represent the critical current of the first and second harmonics respectively. In Josephson junctions formed out of conventional superconducting materials, the second harmonic term and higher terms are negligible. See, Il'ichev *et al.*, 1999, Physical Review B 60, p. 3096, (hereinafter "Il'ichev 1999") which is enclosed as Exhibit A.

The order parameter of a superconducting material determines the properties and characteristics of the superconducting material, and hence the current-phase relationship of weak junctions formed in the material. Conventional superconducting materials have isotropic order parameters. In contrast, unconventional superconducting materials have anisotropic order parameters. See Il'ichev 1999. A common unconventional superconducting material is the d-wave superconductor $\text{YBa}_2\text{Cu}_3\text{O}_{7-x}$ (YBCO), which is used in both Char *et al.* and Il'ichev 1999. The term "d-wave" indicates the type of symmetry of the anisotropic order parameter.

Due to the anisotropy of the d-wave order parameter, the current phase relationship for a Josephson junction in a d-wave superconductor has a temperature dependent second harmonic term. See Il'ichev 1999. The current-phase relationship of the Josephson junctions described in Il'ichev 1999 is:

$$I_p = I'_c \cdot \sin(\varphi) + I''_c \cdot \sin(2\varphi), \quad (2)$$

where I'_c and I''_c are the critical currents of the first and second harmonics respectively. Il'ichev 1999 established that the realized non-sinusoidal behavior in the current-phase relationship of this unconventional superconducting Josephson junction is explained by the presence, and in some cases dominance, of the second harmonic term.

Clean Josephson Junctions

The greater the influence of the second harmonic in the current phase relationship of a Josephson junction, the greater the deviation from conventional 2π periodic

sinusoidal behavior. An unconventional superconductor clean Josephson junction is defined by a current-phase relationship in which the second harmonic makes a distinct contribution to the characteristics of the junction. In terms of Eqn. 2, this is the regime where $I_c'' > I_c' / 2$, which causes the equilibrium state to shift from $\varphi=0$, in the sinusoidal case, to about $\pm\pi/2$, creating a doubly degenerate ground state phase difference across the junction. In other words, the phase differences of about $+\pi/2$ and $-\pi/2$ have equal energy across the unconventional superconductor clean Josephson junction.

As has been described in previous office action responses, the doubly degenerate ground state is an important feature of unconventional superconductor clean Josephson junctions. In the present application, the doubly degenerate ground state is necessary in part to create appropriate operational parameters of the claimed devices. For this reason, the Applicant positively recites the use of a clean Josephson junction and an unconventional superconducting material on at least one side of the clean Josephson junction in each of the pending independent claims.

As seen in Il'ichev 1999, the size of the second harmonic is dependent on a number of factors including temperature. Therefore, the second harmonic can easily be suppressed (e.g., by raising the temperature of the junction). When the second harmonic is suppressed, the junction behaves as a conventional Josephson junction. Parameters such as temperature, size, transparency, and roughness, all make important contributions to this relationship. In particular, it was shown in Il'ichev *et al.*, 1998, Physical Review Letters 81, p. 894, (hereinafter "Il'ichev 1998") which is enclosed as Exhibit B, that for a Josephson junction having width of 2 μ m and operating at a temperature 4.2K, the current phase relationship deviated from the standard sinusoidal behavior. It was further pointed out in Il'ichev 1998 that this was the first observation of non-sinusoidal behavior in a Josephson junction.

In the present invention, the Applicant exploited the dominant second harmonic property of unconventional superconductor clean Josephson junctions to form a useful quantum computing device known as a qubit.

The combination of Tinkham and Char et al. does not teach each and every limitation of the claimed invention.

Char et al. does not teach or suggest clean Josephson Junctions. Based on the art accepted definition of a Josephson junction, the voltage phase relationship of a Char *et al.* device will be sinusoidal in nature if it does not include an unconventional superconducting clean Josephson junction. A comparison of Fig. 15 of Char *et al.* with Fig. 4 of Lindström *et al.*, 2003, Physical Review Letters 90, 117002 (hereinafter “Lindström”) illustrates the difference between conventional Josephson junctions and unconventional superconductor clean Josephson junctions used in devices. Although Char *et al.* describes Josephson junctions formed out of YBCO, an unconventional superconducting material, the resulting voltage phase properties of the devices illustrate conventional behavior, indicating that the second harmonic is suppressed and the Josephson junctions are not in the clean regime. In contrast, Fig. 4 of Lindström examines the same properties of devices that employ unconventional superconductor clean Josephson junctions, and the non-sinusoidal results are quite different from Char *et al.* Lindström is attached as Exhibit C.

As discussed above, Il’ichev 1999 demonstrated that second order harmonics in a Josephson junction formed in a thin layer of YBCO is temperature dependent. Thus, the voltage phase relationship of a Char *et al.* device should adopt a sinusoidal waveform at high temperatures (68K) and adopt a non-sinusoidal waveform at low temperatures (4.2K) if the Char *et al.* device includes a clean Josephson junction. With this in mind, comparison of Fig. 3 of Il’ichev and Fig. 15 of Char *et al.* is instructive. Fig. 3 of Il’ichev 1999 shows how the non-sinusoidal behavior of a Josephson junction capable of exhibiting second harmonic effects is lost as the temperature of the junction is shifted from 4.2K to 40K. In complete contrast, Fig. 15 of Char *et al.* shows that the Char *et al.* device “operates properly” (*i.e.*, exhibits 2π periodic sinusoidal behavior) at temperatures ranging from 4.2K to 77K (see Char *et al.* column 15, lines 35-40). Thus, Char *et al.* describes Josephson junctions for which the second harmonic is suppressed between 4.2K and 77K. This means that Char *et al.* does not teach or suggest clean Josephson junctions.

Tinkham does not teach or suggest unconventional superconductor clean Josephson junctions. Like Char *et al.*, Tinkham does not disclose the use of unconventional superconductor clean Josephson junctions.

In the February 19, 2003 office action, the PTO stated that Tinkham shows a representative small system (*i.e.*, mesoscopic), made up of a small superconducting island connected to charge reservoirs and further, a small superconducting island connected to two macroscopic superconducting leads. The PTO noted that Tinkham does not detail the materials of the island, the leads or the Josephson junctions.

Applicant respectfully points out that Tinkham is only considering conventional superconducting materials in the devices identified by the PTO. In particular, Tinkham does not teach or suggest the use of unconventional superconducting materials in the disclosed devices nor does Tinkham teach or suggest the use of clean Josephson junctions.

Tinkham investigates the properties of a small superconducting island connected to two charge reservoirs via small Josephson junctions (the S-S-S configuration) in the Section entitled “Zero Bias Supercurrents with Superconducting Island and Leads” (Tinkham, p. 274). Equation 7.38a of Tinkham (p. 275) calculates the supercurrent in such devices as:

$$I_s = (2e/\hbar) \cdot E_i \sin(\theta/2), \quad (3)$$

where I_s is the supercurrent, e is the charge of an electron, \hbar is Planck’s constant divided by 2π , and θ is the sum of the phase differences across the two junctions of the device. In the last block of text on page 275, Tinkham comments that this supercurrent equation “... agrees with the classical result for two identical Josephson junctions in series...”.

The supercurrent relation that Tinkham calculates for S-S-S devices indicates that only conventional superconducting materials are being addressed. For example, the current phase relationship that Tinkham calculates depends only on the first harmonic of the phase difference across the Josephson junctions. If Tinkham was considering unconventional superconducting materials in the S-S-S devices identified by the PTO, the current phase relationship in Tinkham would include a second harmonic term as in the case of Il’ichev 1999. Since this term is not present in the current phase relationship for the S-S-S devices identified in Tinkham by the PTO, it is clear that Tinkham only

considers devices consisting of conventional superconducting materials that cannot support unconventional superconductor clean Josephson junctions.

There is no motivation to modify Char et al. or Tinkham to form the claimed devices

In the February 19, 2003 Office Action, the PTO stated that it would have been obvious to provide the best quality crystal structures since this is the standard in semiconductor processing. The Applicant respectfully submits that the practice of providing the best quality crystal structures would not result in the modification of Char *et al.* or Tinkham to include unconventional superconductor clean Josephson junctions. The Applicant has two reasons for this assertion. First, even the best bi-epitaxial technology available at the time the present application was filed could not have achieved the unconventional superconductor clean Josephson junctions recited in the pending claims. Second, even if it were possible to modify Char *et al.* to make the claimed junctions, such junctions would have undesirable electrical characteristics. Because of these undesirable electrical characteristics their use in the conventional electronic devices described in Char *et al.* would result in unsatisfactory device performance. This reasoning is outlined in the following two subsections. Applicant's reasoning is supported by the declaration submitted under 37 C.F.R. § 1.132. However, Applicant's reasoning stands on its own without the support of the declaration.

a. Neither Char et al. nor the best quality crystal structures available for bi-epitaxial Josephson junction technology at the time of filing of the application were sufficiently advanced to prepare an unconventional superconductor clean Josephson junction.

Bi-epitaxial technology involves forming a grain boundary by creating two different substrate regions such that a deposited unconventional superconducting material adopts different crystal orientations depending on the respective substrate region over which it lies. The substrate regions are prepared on a single-crystal substrate and can involve deposition of multiple seed layers in combination with buffer layers and etching stages to form the distinct substrate regions. Although this method provides more flexibility in the creation of grain boundary Josephson junctions than bi-crystal methods, the resulting Josephson junctions are not sufficient to take advantage of some properties

specific to the unconventional superconducting materials, such as the second harmonic described above.

The bi-epitaxial technology described in Char *et al.* illustrates a method for creating conventional Josephson junctions, that is, unconventional superconductor Josephson junctions having a suppressed second harmonic, as described above in detail. The Josephson junctions described in Char *et al.* are not capable of forming the unconventional superconductor clean Josephson junction that is recited in the pending claims.

Further, bi-epitaxial grain boundary Josephson junction technology is complex and intricate, and was not sufficiently advanced at the time of filing of the Application to form unconventional superconductor clean Josephson junctions. Given the difficulties with bi-epitaxial technology at the time the present application was filed, one of skill in the art would not have been able to modify Char *et al.* to produce the devices claimed in the instant application. As such, the combination of Char *et al.* and Tinkham simply cannot provide a motivation to modify such references in order to make the claimed devices.

b. Unpredictability of the second harmonic in unconventional superconductor clean Josephson junctions.

Even if bi-epitaxial technology could be used to make an unconventional superconductor clean Josephson junction, Char *et al.* provides no motivation for making such junctions. As described above, the current-phase relationship of an unconventional superconductor clean Josephson junction has a suppressed first harmonic term and a significant second harmonic term. Fig. 4 of Il'ichev *et al.*, 1999, Physical Review B 60, p. 3096 illustrates that the presence of a significant contribution from the second harmonic term measurably affects the current-phase relationship of the junction. Further, at least in the case of a YBCO thin film with asymmetric 45 degree [001]-tilt grain boundaries, this affect is highly temperature dependent and vanishes at temperatures approaching 30 K. Thus, the use of clean Josephson junctions in the devices of Char *et al.* would introduce an unpredictable non-sinusoidal current-phase dependence in such devices. Since the devices are typically used in applications such as the precise measurement of magnetic fields, this unpredictable current-phase dependence is undesirable.

The unpredictability in the current-phase relationship of such devices, were they to incorporate clean Josephson junctions, would come from at least two sources. First, as illustrated in Il'ichev 1999 (e.g., Figs. 3 and 4), the second harmonic contribution associated with an unconventional superconductor clean Josephson junction is temperature dependent. Second, as detailed in Il'ichev 1999 and in Lindström, state of the art methods for manufacturing unconventional superconductor clean Josephson junctions still have not developed to the point where the strength of the second harmonic can be precisely engineered. Lindström is attached as Exhibit C.

In Il'ichev 1999, bi-crystal YBCO Josephson junction properties were investigated. Films having a thickness of 100 nm were fabricated using standard pulsed laser deposition on (001) oriented SrTiO_3 bi-crystalline substrates with asymmetric [001] tilt misorientation angles $45^\circ \pm 1^\circ$. They were subsequently patterned by argon ion-beam etching into $4 \times 4 \text{ mm}^2$ square washer single-junction interferometer structures as illustrated in Fig. 1 of Il'ichev 1999. Five such samples were studied in Il'ichev 1999 in which the current-phase relation of each of the samples was compared with the current-phase relation of conventional Josephson junctions. Sample No. 1 exhibited the most anomalous (non-sinusoidal) behavior, samples Nos. 2 and 3 were less anomalous and samples Nos. 4 and 5 did not exhibit second order effects whatsoever. See Il'ichev 1999, page 3097, second column, first full paragraph. Thus, even the state of the art methods for manufacturing unconventional superconductor clean Josephson junctions such as Il'ichev 1999 presently fail to make clean Josephson junctions with consistent second order harmonics.

Lindström fabricated SQUIDs from 250 nm thick YBCO-films deposited on SrTiO_3 -bicrystals. The devices were patterned using e-beam lithography and then transferred to a carbon mask employing a multiple step process. Finally, the YBCO was etched through the mask using ion-milling. Lindström reported that the critical current varied from sample to sample (Lindström, page. 2, column 2, third full paragraph). Further, Lindström found that the first order and second order harmonics varied by as much as tens times between the two junctions in each of the manufactured SQUIDs. (Lindström, page. 4, column 1, first paragraph).

The results of Il'ichev 1999 and Lindström show that each unconventional superconductor clean Josephson junction manufactured by such methods would have to be characterized to determine the magnitude of the first and second harmonics. Such a

step is not presently needed in Char *et al.* and there is simply no motivation to alter Char *et al.* to introduce such a step since Char *et al.* does not teach or suggest the use of devices that make use of the second order harmonics of unconventional superconductor clean Josephson junctions.

For the reasons presented above, there is no motivation to alter Char *et al.* in order to make devices that have unconventional superconductor clean Josephson junctions. Likewise, there is no motivation to alter the teachings of Tinkham to incorporate an unconventional superconductor clean Josephson junction. As discussed in detail above, Chapter 7 of Tinkham discusses the Josephson effect in terms of first harmonics only. Incorporation of an unconventional superconductor clean Josephson junction into the structures disclosed in Chapter 7 of Tinkham would be inconsistent with the supercurrent relationship (first order effects only) that Tinkham gives for such S-S-S devices.

For the reasons provided above, Applicant believes that the combination of Tinkham and Char *et al.* does not render obvious claims 1, 3-5, 28, 29, 33, 34, 54, 56, 58, or 60-65. Therefore, the Applicant respectfully requests that the rejection be withdrawn.

Claims 60-63

Claims 60-63 are patentable over the combination of Tinkham and Char *et al.* for the additional reason that neither reference teaches or suggests the form of quantum tunneling recited in these claims. Claim 60 recites a supercurrent that tunnels between a first ground state and a second ground state. Tinkham and Char *et al.*, or any combination of Tinkham and Char *et al.*, do not teach or suggest an unconventional superconductor clean Josephson junction between a mesoscopic island and a bank. As described above, the unconventional superconductor clean Josephson junctions introduces ground states with about a $\pm \pi/2$ phase difference across the junction. Each of these phase differences have the same energy, and hence are degenerate, permitting quantum tunneling when the elements of the claims are realized. For this reason, the cited references fail to disclose a Josephson junction that is configured so that a supercurrent proximate to the Josephson junction alternates between a first ground state having a first magnetic moment and a second ground state having a second magnetic moment by means of quantum tunneling as recited in claim 60. Claims 61-63 depend from claim 60 and therefore are not rendered obvious by the combination of Char *et al.* and Tinkham for the same reasons.

Claims 2, 30, 31, and 52

The PTO has rejected claims 2, 30, 31, and 52 under 35 U.S.C. 103(a) as being unpatentable over Tinkham in view of Char *et al.* (USP 5,157,466) and further in view of Shnirman *et al.*

Tinkham, either alone or in combination with Char *et al.*, does not teach or suggest claims 1, 28, 60 or 64 for the reasons discussed above. Shnirman merely teaches a SET capacitively coupled to a Josephson junction qubit. As such, Shnirman *et al.* does not remedy the deficiencies identified in Tinkham and Char *et al.*. For this reason, the combination of Tinkham, Char *et al.*, and Shnirman *et al.* does not render claims 1, 28, 60 or 64 obvious. Since claims 2, 30, 31, and 52 ultimately depend from 1, 28, 60 or 64, the cited references do not anticipate these claims either. Accordingly, Applicant respectfully requests that the rejection be withdrawn.

Claims 6, 8-10, 35, 39, 40, 41, 53, 55, 57, and 59

The PTO has rejected claims 6, 8-10, 35, 39, 40, 41, 53, 55, 57, and 59 under 35 U.S.C. 103(a) as being unpatentable over Tinkham in view of Char *et al.* (USP 5,157,466) and further in view of Baechtold *et al.* (USP 3,953,749). Tinkham, either alone or in combination with Char *et al.*, does not anticipate claims 1, 28, 60 or 64 for the reasons discussed above. Baechtold *et al.* merely teaches a binary circuit consisting of a series/parallel arrangement of Josephson junctions. As such, Baechtold *et al.* does not remedy the deficiencies identified in the combination of Tinkham and Char *et al.*. For this reason, the combination of Tinkham, Char *et al.*, and Baechtold *et al.* does not render claims 1, 28, 60 or 64 obvious. Since claims 6, 8-10, 35, 39, 40, 41, 53, 55, 57, and 59 ultimately depend from 1, 28, 60 or 64, the cited references do not anticipate these claims either. Accordingly, Applicant respectfully requests that the rejection be withdrawn.

Claims 7, 11, 12-18, 36, 37, 42, 43, 45, 46, and 48-50

The PTO has rejected claims 7, 11, 12-18, 36, 37, 42, 43, 45, 46, and 48-50 under 35 U.S.C. 103(a) as being unpatentable over Tinkham in view of Char *et al.*, Baechtold *et al.* and further in view of Shnirman *et al.* As previously discussed, Tinkham, either alone or in combination with Char *et al.*, does not anticipate claims 1, 28, 60 or 64. Baechtold *et al.* and Shnirman *et al.* do not remedy the deficiencies identified in the combination of

Tinkham and Char *et al.* For this reason, the cited references, either alone or in any combination, do not render claims 1, 28, 60 or 64 obvious. Since claims 7, 11, 12-18, 36, 37, 42, 43, 45, 46, and 48-50 ultimately depend from claims 1, 28, 60 or 64, the references do not anticipate these claims either. Accordingly, Applicant respectfully requests that the rejection be withdrawn.

DOUBLE PATENTING REJECTION

The PTO has rejected claims 1-18 and 28-65 under the judicially created doctrine of obviousness-type double patenting as being unpatentable over claims 1-6, 12, 14, 15, and 18-25 of U.S. Patent No. 6,459,097 in view of Char *et al.* Although the Applicant disagrees with the PTO's reasoning, in order to expedite prosecution, the Applicant has authorized the enclosed terminal disclaimer.

CONCLUSION

In light of the above remarks, the Applicant respectfully requests that the PTO reconsider this application with a view towards allowance. The PTO is invited to call the undersigned attorney if a telephone call could help resolve any remaining items.

Respectfully submitted,

PENNIE & EDMONDS LLP

By: 

Gary S. Williams
Reg. No. 31,066

3300 Hillview Avenue
Palo Alto, CA 94304
Telephone: (650) 493-4935

APPENDIX A
AMENDED CLAIM

3. (Amended) The structure of claim 1, wherein the clean Josephson junction comprises a grain boundary between the bank and the island.

65. (Amended) A quantum computer comprising the quantum register of claim 64 and a readout device for detecting whether the supercurrent of each clean Josephson junction has the first magnetic moment or the second magnetic moment.

EXHIBIT A

Il'ichev *et al.*, 1999, Physical Review B 60, 3096

Anomalous periodicity of the current-phase relationship of grain-boundary Josephson junctions in high- T_c superconductors

E. Il'ichev, V. Zakosarenko, R. P. J. IJsselsteijn, H. E. Hoenig, V. Schultze, and H.-G. Meyer

Department of Cryoelectronics, Institute for Physical High Technology, P.O. Box 100239, D-07702 Jena, Germany

M. Grajcar and R. Hlubina

Department of Solid State Physics, Comenius University, Mlynská Dolina F2, 842 15 Bratislava, Slovakia

(Received 28 January 1999)

The current-phase relation (CPR) for asymmetric 45° Josephson junctions between two d -wave superconductors has been predicted to exhibit an anomalous periodicity. We have used the single-junction interferometer to investigate the CPR for these kinds of junctions in $\text{YBa}_2\text{Cu}_3\text{O}_{7-\delta}$ thin films. A remarkable amplitude of the π -periodical component of the CPR has been experimentally found, providing an additional source of evidence for the d -wave symmetry of the pairing state of the cuprates. [S0163-1829(99)05629-5]

A number of experimental results confirm d_{12} -wave symmetry of the pairing state of high-temperature superconductors.¹ An unconventional pairing state requires the existence of zeros of the order parameter in certain directions in momentum space. Thermodynamic and spectroscopic measurements do indeed suggest their existence, but by themselves they do not exclude conventional s -wave pairing with nodes.¹ Direct evidence for the d -wave pairing state is provided by phase-sensitive experiments, which are based on the Josephson effect.² Quite generally, the current-phase relationship (CPR) of a Josephson junction, $I(\varphi)$ is an odd periodic function of φ with a period 2π .³ Therefore $I(\varphi)$ can be expanded in a Fourier series

$$I(\varphi) = I_1 \sin \varphi + I_2 \sin 2\varphi + \dots \quad (1)$$

In the tunnel limit we can restrict ourselves to the first two terms in Eq. (1). Since the order parameter is bound to the crystal lattice, $I(\varphi)$ of a weak link depends on the orientation of the d -wave electrodes with respect to their boundary. The existing phase-sensitive experiments exploit possible sign changes of I_1 between different geometries.² In this work we present a phase-sensitive experimental test of the pairing state symmetry of cuprates. Namely, in certain geometries, the I_1 term should vanish by symmetry. In such cases, the CPR should exhibit an anomalous periodicity.

Let us analyze the angular dependence of $I_{1,2}$ in a junction between two macroscopically tetragonal d -wave superconductors. As emphasized in Ref. 4, also heavily twinned orthorhombic materials such as $\text{YBa}_2\text{Cu}_3\text{O}_{7-\delta}$ belong to this class, if the twin boundaries have odd symmetry. We consider an ideally flat interface between two superconducting electrodes. Let θ_1 (θ_2) denote the angle between the normal to the grain boundary and the a axis in electrode 1 (2), see Fig. 1. If we only keep the lowest-order angular harmonics, the symmetry of the problem dictates that⁴

$$I_1 = I_c \cos 2\theta_1 \cos 2\theta_2 + I_s \sin 2\theta_1 \sin 2\theta_2. \quad (2)$$

The coefficients I_c, I_s are functions of the barrier strength, temperature T , etc. The I_2 term results from higher-order tunneling processes and we neglect its weak angular dependence. It is seen from Eq. (2) that the criterion for the observation of an anomalous period of the CPR, $I_1 = 0$, is realized for an asymmetric 45° junction, i.e., a junction with $\theta_1 = 45^\circ$ and $\theta_2 = 0$.

The I_2 term is also present in weak links based on conventional s -wave superconductors but for all known types of weak links $|I_2/I_1| < 1$. For instance, for a tunnel junction $|I_2/I_1| \ll 1$. For a superconductor normal-metal superconductor (SNS) junction, $I \propto \sin \varphi/2$ at $T = 0$,⁵ and the Fourier expansion of Eq. (1) leads to $I_2/I_1 = -2/5$. Therefore a possible experimental observation of $|I_2/I_1| \gg 1$ in an asymmetric 45° junction provides direct evidence of d -wave symmetry of the pairing state in the cuprates.

We have investigated the CPR of $\text{YBa}_2\text{Cu}_3\text{O}_{7-\delta}$ thin-film bicrystals with asymmetric 45° [001]-tilt grain boundaries as sketched in Fig. 1, using a single-junction interferometer configuration in which the Josephson junction is inserted into a superconducting loop with a small inductance L . In a stationary state without fluctuations, the phase difference φ across the junction is controlled by applying an external magnetic flux Φ_e penetrating the loop: $\varphi = \varphi_e - \beta f(\varphi)$. Here $\varphi_e = 2\pi\Phi_e/\Phi_0$; $\Phi_0 = 2.07 \times 10^{-15} \text{ Tm}^2$ is the flux quantum; $f(\varphi) = I(\varphi)/I_0$ is the CPR normalized to the maximal Josephson current I_0 , and $\beta = 2\pi L I_0/\Phi_0$ is the normalized

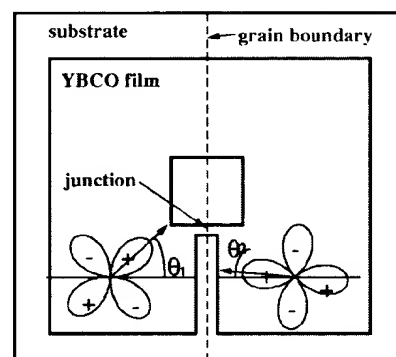


FIG. 1. Washer-shaped interferometer with one short Josephson junction (not in scale). Dimensions are given in the text.

critical current. In order to obtain the CPR for the complete phase range $-\pi \leq \varphi \leq \pi$ the condition $\beta < 1$ has to be fulfilled, because for $\beta > 1$ the curve $\varphi(\varphi_c)$ becomes multivalued. Following Ref. 3, we express the effective inductance of the interferometer using the derivative f' with respect to φ as $L_{int} = L[1 + 1/\beta f'(\varphi)]$. The inductance can be probed by coupling the interferometer to a tank circuit with inductance L_T , quality factor Q , and resonance frequency ω_0 through the mutual inductance M .⁸ External flux in the interferometer is produced by a current $I_{dc} + I_{rf}$ in the tank coil and can be expressed as $\varphi_c = 2\pi(I_{dc} + I_{rf})M/\Phi_0 = \varphi_{dc} + \varphi_{rf}$, where $M^2 = k^2 L L_T$ with k a coupling coefficient. Taking into account the quasiparticle current in the presence of a voltage V across the junction the phase difference is given by the relation $\varphi = \varphi_{dc} + \varphi_{rf} - \beta f'(\varphi) - 2\pi\tau(\varphi)V/\Phi_0$, where $\tau(\varphi) = L/R_J(\varphi)$ with $R_J(\varphi)$ the resistance of the junction. In the small-signal limit $\varphi_{rf} \ll 1$ and in the adiabatic case $\omega\tau \ll 1$, keeping only the first-order terms, the effective inductance L_{eff} of the tank circuit-interferometer system is

$$L_{eff} = L_T \left(1 - k^2 \frac{L}{L_{int}} \right) = L_T \left(1 - \frac{k^2 \beta f'(\varphi)}{1 + \beta f'(\varphi)} \right).$$

Thus the phase angle α between the driving current and the tank voltage U at the resonance frequency of the tank circuit ω_0 is

$$\tan \alpha(\varphi) = \frac{k^2 Q \beta f'(\varphi)}{1 + \beta f'(\varphi)}. \quad (3)$$

Using the relation $[1 + \beta f'(\varphi)]d\varphi = d\varphi_{dc}$ which is valid for $\varphi_{rf} \ll 1$ and $\omega\tau \ll 1$, one can find the CPR from Eq. (3) by numerical integration.

The advantage of the CPR measurement of an asymmetric 45° junction with respect to the by-now standard phase-sensitive tests of pairing symmetry based on the angular dependence of I_1 is twofold. First, it avoids the complications of the analysis of experiments caused by the presence of the term I_3 .⁴ Second, flux trapped in the interferometer washer (see Fig. 1) does not invalidate the conclusions about the ratio $|I_2/I_1|$ and hence about the pairing symmetry, which is not the case in standard phase-sensitive tests of the *d*-wave symmetry of the pairing state.⁹

The films of 100-nm thickness were fabricated using standard pulsed laser deposition on (001) oriented SrTiO₃ bicrystalline substrates with asymmetric [001] tilt misorientation angles of 45° ± 1°. The films were subsequently patterned by Ar ion-beam etching into 4 × 4-mm² square washer single-junction interferometer structures (Fig. 1). The widths of the junctions were 1–2 μm. The square washer holes had a side length of 50 μm. This geometry of the interferometer gives $L \approx 80 \mu\text{H}$. The resistance of a similar single junction (without interferometer loop) was measured directly and $R_J > 1 \Omega$ was found. Therefore the condition for the adiabatic limit $\omega\tau \ll 1$ is satisfied. For measurements of $\alpha(\varphi_{dc})$, several tank circuits with inductances 0.2–0.8 μH and resonance frequencies 16–35 MHz have been used. The unloaded quality factor of the tank circuits $70 < Q < 150$ has been measured at various temperatures. The coupling factor k was determined from the period ΔI_{dc} of $\alpha(I_{dc})$ using $M\Delta I_{dc} = \Phi_0$. Its value varied between 0.03 and 0.09. The

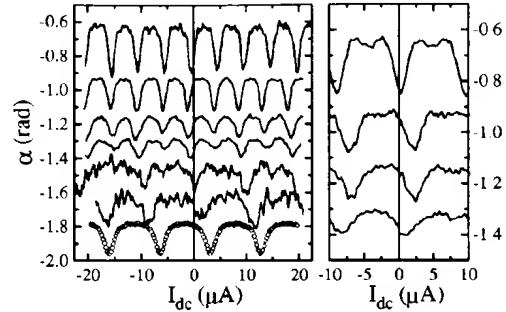


FIG. 2. Left panel: Phase angle between the driving current and the output voltage measured for sample No. 1 at different temperatures as a function of the dc current I_{dc} . The curves are shifted along the y axis and the data for $T = 30$ and 40 K are multiplied by factor 4 for clarity. From top to bottom, the data correspond to $T = 4.2, 10, 15, 20, 30$, and 40 K. The data measured for 36° bicrystals ($\theta_1 \approx 36^\circ, \theta_2 \approx 0$) at $T = 40$ K in the same washer geometry are shown for comparison (open circles). Right panel: The same for sample No. 3. From top to bottom, the data correspond to $T = 4.2, 10, 15$, and 20 K.

amplitude of I_{rf} was set to produce a flux in the interferometer smaller than $0.1 \Phi_0$ to ensure the small-signal limit.

The measurements have been performed in a gas-flow cryostat with a five-layer magnetic shielding in the temperature range $4.2 \leq T \leq 90$ K. The experimental setup was calibrated by measuring interferometers of the same size with 24° and 36° grain boundaries. We have studied six samples, out of which for four samples the π -periodic component of $I(\varphi)$ was experimentally observed. At low temperatures for two samples (Nos. 1 and 2) the value of I_2 is larger than I_1 . For sample Nos. 3 and 4 I_2 is approximately 10–20% of I_1 and for sample Nos. 5 and 6 I_2 is negligible. As an example we plot the phase angle α as a function of the dc current I_{dc} for sample Nos. 1 and 3 (Fig. 2). The behavior of sample No. 1 at low temperatures is defined by the π periodic component of $I(\varphi)$. The curves for sample No. 3 are 2 π -periodic, nevertheless for the curve at $T = 4.2$ K the local minima clearly show the presence of a π -periodic component.

In order to determine the CPR we assume that the period of $\alpha(I_{dc})$ at $T = 40$ K and $\Delta I_{dc} = 9.6 \mu\text{A}$, corresponds to $\Delta\varphi_{dc} = 2\pi$. We take $\varphi_{dc} = 0$ at a maximum or minimum of α . This is necessary in order to satisfy $I(\varphi = 0) = 0$, as required by general principles.³ The experimentally observed shift of the first extreme of $\alpha(I_{dc})$ from $I_{dc} = 0$ (Fig. 2) can be due to flux trapped in the interferometer washer. Most probably, this flux resides in the long junction originated by the grain boundary crossing the washer of the interferometer. This long junction does not play an active role because the Josephson penetration depth is much smaller than the junction length, and external fields produced by I_{dc} are smaller than the first critical field. Nevertheless, the long junction sets the phase difference for $I_{dc} = 0$ at the small junction.

In Fig. 3, we show the CPR determined from the data in Fig. 2. For all curves we have performed a minimal necessary shift consistent with $I(\varphi = 0) = 0$. Thus we have assumed that at $\varphi_{dc} = 0$ a minimum of $\alpha(\varphi_{dc})$ is realized. For an interferometer with a conventional *s*-wave weak link (and also for the 36° junction), at $\varphi_{dc} = 0$ one gets a maximum of

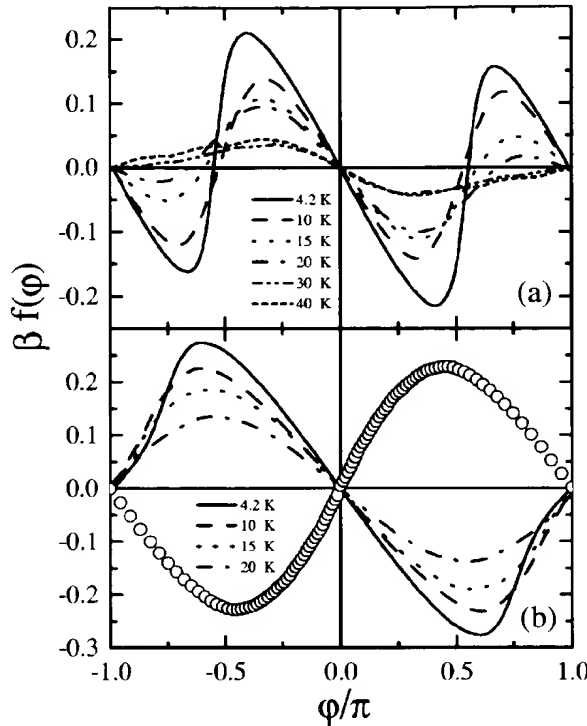


FIG. 3. (a) Josephson current through the junction for sample No. 1 as a function of the phase difference φ , determined from the data in Fig. 2. The scattering of $\alpha(\varphi)$ values was reduced by folding the data back to the interval $\langle 0, \pi \rangle$ and taking the average. Here, the symmetry $\alpha(\varphi) = \alpha(-\varphi)$ was assumed. (b) The same for sample No. 3. The data for the asymmetric 36° bicrystal at $T = 40$ K (open circles) are also shown.

$\alpha(\varphi_{dc})$. Note that the minimum of $\alpha(\varphi_{dc})$ at $\varphi_{dc} = 0$ implies a paramagnetic response of the interferometer in the limit of small applied fields.

The amplitude of the π -periodic component of the CPR decreases drastically with increasing temperature, and at $T = 40$ K its contribution is negligible for all samples. The temperature dependence of I_1 and I_2 could be determined with acceptable accuracy for sample No. 1 only. With decreasing T , $|I_2|$ grows monotonically down to $T = 4.2$ K, while the I_1 component exhibits only a weak temperature dependence (Fig. 4).

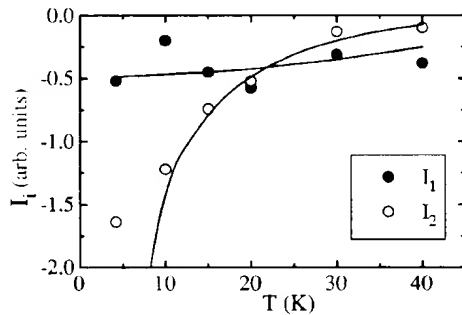


FIG. 4. Temperature dependence of the Fourier expansion coefficients $I_{1,2}$ determined from the experimental data in Fig. 3(a). Solid lines are the Fourier expansion coefficients for the numerical data in Fig. 5.

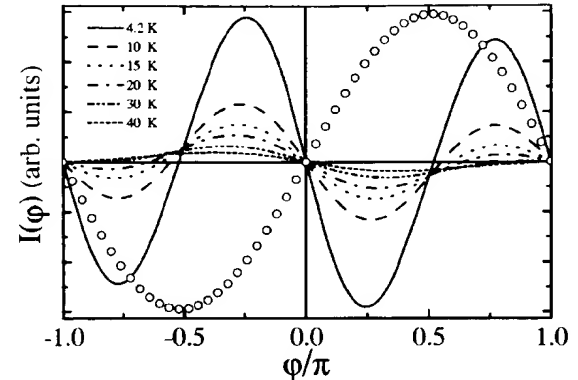


FIG. 5. $I(\varphi)$ calculated according to Eq. (64) of Ref. 11 for a junction with $\theta_1 = 45.5^\circ$, $\theta_2 = 0$, $\lambda d = 1.5$, $\kappa = 0.5$, and $T_c = 60$ K. $I(\varphi)$ at $T = 40$ K for the 36° bicrystal (open circles) was calculated with the same parameters except for $\theta_1 = 36^\circ$.

Our experimental results can be understood as follows. It is well known that the microstructural properties of the grain boundaries, especially 45° boundaries, are defined by their faceted nature. Faceting is an intrinsic property of the grain boundaries,^{6,7} and, due to d -wave symmetry of the order parameter, the properties of the junctions strongly depend on the particular distribution of the facets. Small deviations from the ideal geometry of the asymmetric 45° junction lead to a finite value of I_1 . Thus for nearly ideal junctions $|I_2/I_1| \gg 1$ at $T \rightarrow 0$. The region $T \sim T_c$ can be analyzed quite generally within the Ginzburg-Landau theory. Let the electrodes be described by the (macroscopic) order parameters $\Delta_{1,2} = |\Delta| e^{i\varphi_{1,2}}$. Then the phase-dependent part of the energy of the junction is $E = a[\Delta_1 \Delta_2^* + \text{H.c.}] + b[(\Delta_1 \Delta_2^*)^2 + \text{H.c.}] + \dots$ where a, b, \dots depend weakly on T .¹⁰ Thus for T close to T_c we estimate $I_1 \propto |\Delta|^2 \propto (T_c - T)$ and $I_2 \propto |\Delta|^4 \propto (T_c - T)^2$, leading to $|I_2/I_1| \ll 1$. With increasing deviations from ideal geometry $|I_2/I_1|$ decreases. For large enough deviations, negligible values of $|I_2|$ are expected. These expectations are qualitatively consistent with the experimental data (see also Fig. 4).

So far, our discussion was based solely on symmetry arguments. Let us attempt a more quantitative analysis of our data now. Two different microscopic pictures of asymmetric 45° Josephson junctions between d -wave superconductors have been considered in the literature. The first picture assumes a microscopically tetragonal material and an ideally flat interface.¹⁰⁻¹² Within this picture, only sample No. 1 can be analyzed. Sample No. 2 had $I_0(T = 1.5$ K) $\approx 10^{-2} \mu\text{A}$. At this temperature only the π -periodic component of $I(\varphi)$ was observed. At higher temperatures I_0 was not measurable. $I(\varphi)$ for sample No. 1 calculated according to the model of Ref. 11 is shown in Fig. 5. The experimental data can be fitted within a relatively broad range of barrier heights. However, if we require the $I(\varphi)$ relation of the 36° junction to be fitted by the same (or smaller) barrier height as for the 45° junction, we conclude the barrier of the 45° junction to be rather low.¹⁴ The dependence of $I(\varphi)$ on T requires a choice of $T_c \approx 60$ K in the non-self-consistent theory of Ref. 11. The reduction from the bulk $T_c = 90$ K is probably due to a combined effect of surface degradation and order-parameter suppression at the sample surface. The temperature dependence

of the ratio of the π and 2π periodic components in $I(\varphi)$ is seen to be in qualitative agreement with experimental data in Fig. 3(a). This is explicitly demonstrated in Fig. 4 where we compare the experimentally obtained $I_{1,2}$ with the results of the Fourier analysis of the curves in Fig. 5. The divergence of I_2 as $T \rightarrow 0$ is an artifact of the ideal junction geometry assumed in Ref. 11. If a finite roughness of the interface is taken into account, this divergence is cut off and the experimental data in Fig. 4 do indeed resemble theoretical predictions for a rough interface.¹² However, the non-self-consistent theory of Ref. 11 is unable to explain the experimentally observed steep CPR close to the minima of the junction energy [see Fig. 3(a)].

In a different approach a heavily meandering interface with $\theta_i = \theta_i(x)$ is assumed. Now, the critical current density $j_c(x)$ is a random function with a typical amplitude $\langle |j_c(x)| \rangle \sim j_c$. If the average critical current along the junction $\langle j_c \rangle < j_c$, a remarkable π -periodic component is present in the CPR. The relation $|I_2/I_1|$ depends on the distribution of $j_c(x)$ and can be much larger than one for $\langle j_c \rangle \ll j_c$.^{15,16} This model qualitatively explains the obtained results for all samples, however for a quantitative comparison the actual microscopic distribution $j_c(x)$ should be known. Note that

also within the picture of Refs. 15 and 16 the d -wave symmetry of the pairing state is crucial, otherwise the condition $\langle j_c \rangle \ll j_c$ is difficult to satisfy.

Our present understanding of $I(\varphi)$ in the asymmetric 45° junction is only qualitative. We cannot say whether the remarkable amplitude of the π -periodic component of $I(\varphi)$ is dominated by the microscopically flat regions,¹³ or due to the spatial inhomogeneity of the junction. This issue requires further study.

In conclusion, we have measured the magnetic-field response of a single-junction interferometer based on asymmetric 45° grain-boundary junctions in $\text{YBa}_2\text{Cu}_3\text{O}_{7-\delta}$ thin films. A large π -periodic component of $I(\varphi)$ has been experimentally found, which is in agreement with theoretical predictions for $d_{x^2-y^2}$ -wave superconductors. Hence our results provide an additional source of evidence for the d -wave symmetry of the pairing state in the cuprates.

Financial support by the DFG (Ho 461/3-1) and partial support by INTAS (N 11459) are gratefully acknowledged. M. G. and R. H. were supported by the Slovak Grant Agency (Grant No. 1/4300/97) and the Comenius University (Grant No. UK/3927/98).

¹ For a review, see J. Annett, N. Goldenfeld, and A. J. Leggett, in *Physical Properties of High Temperature Superconductors*, edited by D. M. Ginsberg (World Scientific, New Jersey, 1996), Vol. V.

² See C. C. Tsuei *et al.*, Science **271**, 329 (1996), and references therein.

³ A. Barone and G. Paterno, *Physics and Applications of the Josephson Effect* (Wiley, New York, 1982).

⁴ M. B. Walker and J. Luettmmer-Strathmann, Phys. Rev. B **54**, 588 (1996).

⁵ I. O. Kulik and A. N. Omel'yanchuk, Fiz. Nizk. Temp. **4**, 296 (1978) [Sov. J. Low Temp. Phys. **4**, 142 (1978)].

⁶ H. Hilgenkamp, J. Mannhart, and B. Mayer, Phys. Rev. B **53**, 14 586 (1996).

⁷ J. Mannhart *et al.*, Phys. Rev. Lett. **77**, 2782 (1996).

⁸ E. V. Il'ichev *et al.*, J. Low Temp. Phys. **106**, 503 (1997).

⁹ R. A. Klemm, Phys. Rev. Lett. **73**, 1871 (1994).

¹⁰ A. Huck, A. van Otterlo, and M. Sigrist, Phys. Rev. B **56**, 14 163 (1997).

¹¹ Y. Tanaka and S. Kashiwaya, Phys. Rev. B **56**, 892 (1997).

¹² Y. S. Barash, H. Burkhardt, and D. Rainer, Phys. Rev. Lett. **77**, 4070 (1996).

¹³ C. R. Hu, Phys. Rev. Lett. **72**, 1526 (1994).

¹⁴ This is consistent with the Fourier analysis of the data in Fig. 3 which results in a non-negligible I_n also for $n \geq 3$.

¹⁵ A. J. Millis, Phys. Rev. B **49**, 15 408 (1994).

¹⁶ R. G. Mints, Phys. Rev. B **57**, R3221 (1998).

EXHIBIT B

Il'ichev *et al.*, 1998, Physical Review Letters 81, p. 894

Nonsinusoidal Current-Phase Relationship of Grain Boundary Josephson Junctions in High- T_c Superconductors

E. Il'ichev, V. Zaksarenko, R. P. J. IJsselsteijn, V. Schultze, H.-G. Meyer, and H. E. Hoenig

Department of Cryoelectronics, Institute for Physical High Technology, P.O. Box 100239, D-07702 Jena, Germany

H. Hilgenkamp and J. Mannhart

Experimental Physics VI, Center for Electronic Correlations and Magnetism, Institute of Physics, Augsburg University, D-86135 Augsburg, Germany

(Received 13 January 1998)

For various configurations of Josephson junctions incorporating superconductors with unconventional order parameter symmetry, such as most high- T_c cuprates, deviations from the standard sinusoidal current-phase dependence have been predicted. To this point, these deviations have never been observed experimentally. We have measured the current-phase relation of high- T_c Josephson junctions, namely, $\text{YBa}_2\text{Cu}_3\text{O}_{7-x}$ thin film bicrystals, comprising symmetric 45° [001] tilt grain boundaries. The current-phase relations of all junctions investigated were found to be extremely nonharmonic, in agreement with a $d_{x^2-y^2}$ -wave dominated symmetry of the order parameter. [S0031-9007(98)06674-5]

PACS numbers: 74.50.+r

The current-phase relation (CPR) $f(\varphi)$ is a characteristic property of any weak link connecting two superconductors. It describes the dependence of the Cooper-pair current I_p on the phase difference φ of the order parameters of both superconducting electrodes. In a general form it is expressed as

$$I_p = I_c f(\varphi), \quad -1 \leq f(\varphi) \leq 1, \quad (1)$$

I_c being the critical current of the weak link. It was shown by Josephson [1] that for ideal tunnel junctions between conventional superconductors the CPR is sinusoidal, i.e., $f(\varphi) = \sin(\varphi)$. This sinusoidal dependence has been confirmed experimentally numerous times for standard tunnel junctions between conventional superconductors [2].

Recently, it has been revealed that the order parameter of most high- T_c cuprates is unconventional, dominated by a $d_{x^2-y^2}$ symmetry component [3–5]. Because of the sign change of the order parameter associated with this symmetry, strong deviations from the standard sinusoidal dependence have been predicted for the current-phase relations of various configurations of Josephson junctions employing such unconventional superconductors [6–9]. In particular, nonharmonic and double-periodic current-phase relations are expected for junctions oriented nominally perpendicular to the $\langle 110 \rangle$ direction of one or of both electrodes, as well as for junctions for which the $\langle 110 \rangle$ direction of one of the electrodes is aligned with the $\langle 100 \rangle$ direction of the other, such as for 45° [001] tilt grain boundaries.

These predictions are highly unusual. Therefore, an experimental clarification of the CPR for high- T_c junctions for which deviations from a standard harmonic behavior are expected is desirable. Such experiments will further

enhance the understanding of the influence of the order parameter symmetry on the properties of grain boundaries and high- T_c Josephson junctions. In addition, they will provide valuable information for the design and use of Josephson junction-based circuits, of which many characteristics directly depend on the CPR. However, to our knowledge, such experiments have not been carried out. All available data refer to Josephson junctions for which nominally sinusoidal current-phase relations are expected. The CPR was measured for weak links prepared by ion irradiation [10], for step-edge junctions [11,12], and also for 24° bicrystal grain boundaries [12]. In nearly all of these cases sinusoidal current-phase relations were found. Deviations from a sinusoidal dependence have been observed only for one step-edge junction, measured at 77 K [12]. These deviations can be explained by the influence of thermal noise [13].

For these reasons we have investigated the CPR of $\text{YBa}_2\text{Cu}_3\text{O}_{7-x}$ thin film bicrystals with symmetric 45° [001]-tilt grain boundaries, as sketched in Fig. 1(a). For these junctions, strong deviations from a sinusoidal CPR are anticipated.

Following a standard approach [14], the CPR was measured using a single-junction interferometer configuration in which the Josephson junction is part of a superconducting loop with a small inductance L . The phase difference φ across the junction is controlled by applying an external magnetic flux Φ_e penetrating the loop:

$$\varphi = \varphi_e - \beta f(\varphi) + \varphi_n + 2\pi m. \quad (2)$$

Here, $\varphi_e = 2\pi\Phi_e/\Phi_0$ is the external flux normalized to the flux quantum Φ_0 ($= 2.07 \times 10^{-15} \text{ Tm}^2$). The constant $\beta = 2\pi L I_c / \Phi_0$ is the normalized critical current, φ_n is a term accounting for the effective noise, and m is

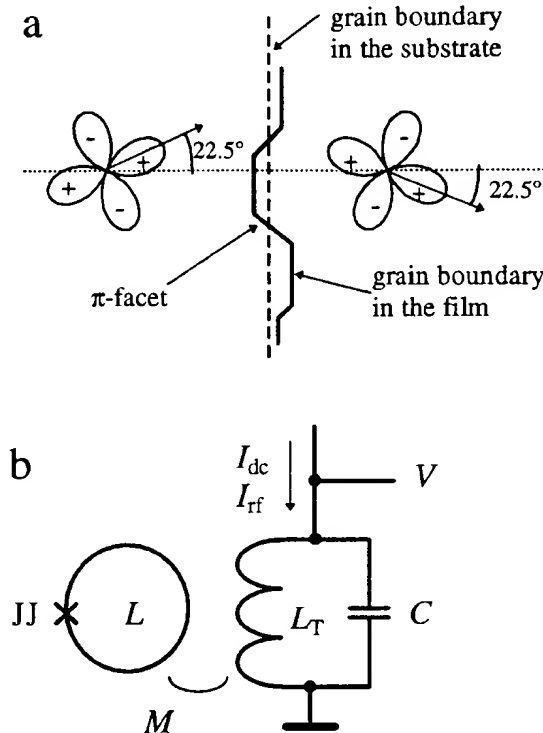


FIG. 1. (a) Schematic representation of a symmetric 45° [001]-tilt grain boundary junction in a d_{3-32} superconductor. The boundary in the superconducting thin film is meandering, leading to the occurrence of π facets. (b) Schematic of the measurement setup. The Josephson junction is denoted by JJ, and C indicates the capacitance of the tank circuit. The other denotations are explained in the text.

an integer. As capacitive contributions to the loop current are insignificant at the measurement frequencies, the junction capacitance has been neglected. The quasiparticle current is also negligible, for reasons discussed below.

The superconducting loop is inductively coupled to a tank circuit with inductance L_T [see Fig. 1(b)]. This tank circuit is driven with a current I_{rf} at a frequency ω and a dc current I_{dc} . Thus, φ_e can be expressed as a sum of a dc and an rf component $\varphi_e = \varphi_{dc} + \varphi_{rf}$. In this arrangement, the effective impedance $Z_{\text{eff}}(\omega)$ of the loop-tank circuit combination is a function of φ_e . As shown by Rifkin and Deaver [14], the CPR can be obtained from this dependence, provided that $\varphi_{rf} \ll 1$. To obtain the CPR for the complete phase range $0 \leq \varphi \leq 2\pi$, the condition $\beta < 1$ has to be fulfilled in addition.

To enhance the accuracy of the measurement, we have adapted this common approach and retrieved the CPR from a measurement of the φ_{dc} dependence of the phase angle α between the drive current I_{rf} and the tank voltage V at the resonant frequency of the tank circuit ω_0 . As described in Ref. [12], at ω_0 , the $\alpha(\varphi_{dc})$ dependence is related to the derivative of the CPR $f'(\varphi) \equiv df(\varphi)/d\varphi$ in the following way:

$$\tan \alpha(\varphi_{dc}) = \frac{k^2 Q \beta f'(\varphi(\varphi_{dc}))}{1 + \beta f'(\varphi(\varphi_{dc}))}. \quad (3)$$

Here k is the coupling factor between the tank inductance and the interferometer, $k^2 = M^2/(LL_T)$, where M is the mutual inductance [Fig. 1(b)]. Using Eq. (3), from the measured $\alpha(\varphi_{dc})$ dependence $f'(\varphi(\varphi_{dc}))$ is obtained. The CPR is restored by integrating $f'(\varphi(\varphi_{dc}))$ numerically, using the $d\varphi(\varphi_{dc})/d\varphi_{dc}$ dependence obtained from differentiating Eq. (2) with respect to φ_{dc} .

The samples investigated consisted of three bicrystalline $\text{YBa}_2\text{Cu}_3\text{O}_{7-x}$ films with a T_c ($R = 0$) of 88 K. The films, with thickness $t = 100$ nm, were deposited by standard pulsed laser deposition on (001)-oriented SrTiO_3 bicrystalline substrates [15] with symmetric [001]-tilt misorientation angles of $45^\circ \pm 2^\circ$ and were subsequently patterned by Ar ion-beam etching into $8 \times 8 \text{ mm}^2$ or $5 \times 5 \text{ mm}^2$ square washer single-junction interferometer structures. The widths of the junctions were $b \approx 2-3 \mu\text{m}$. The washer holes had a side length of $50 \mu\text{m}$, leading to $L \approx 80 \text{ pH}$.

To minimize the influence of external noise, the samples were measured in superconducting and double magnetic shielding at a temperature of 4.2 K. The condition $\beta < 1$ for the investigated interferometers was confirmed experimentally from the character of its response versus φ_{dc} [12].

$\text{YBa}_2\text{Cu}_3\text{O}_{7-x}$ grain boundaries with a symmetric [001] tilt angle of 45° typically have a normal-state interface-resistivity $\rho_n > 1 \times 10^{-8} \Omega \text{ cm}^2$, which we also measured for boundaries fabricated under identical conditions as the junctions used in the present experiments. In the configuration used, this ρ_n corresponds to normal-state resistances $R_n > 1 \Omega$. Accordingly, the relaxation time of the interferometer $\tau = L/R$ is short ($\tau \ll 1/\omega_0$), and hence the quasiparticle current is negligible [12].

For the measurements of $\alpha(\varphi_{dc})$, two tank circuits with quality factor $Q = 120$ and inductance $L_T = 0.4 \mu\text{H}$, $\omega_0 = 30 \text{ MHz}$, and $L_T = 0.73 \mu\text{H}$, $\omega_0 = 23 \text{ MHz}$, respectively, were employed. The phase angle was recorded as a function of I_{dc} after amplification of the tank voltage by a high-impedance amplifier. The coupling coefficient k was determined from the period of the $\alpha(I_{dc})$ dependence. Values of $k = 0.072$ and $k = 0.054$ for the respective tank circuits are obtained. To ensure the validity of the small-signal limit, the measurements were carried out with $\varphi_{rf} < 0.15$.

A typical $\alpha(I_{dc})$ dependence is shown in Fig. 2. The corresponding CPR, depicted in Fig. 3, is clearly deviating from the standard sinusoidal behavior. Samples fabricated on different substrates and measured with both tank coils followed closely the same behavior. It is emphasized that the experimental setup employed and the procedure followed are identical to those used to measure the current-phase relations of step-edge junctions and thin-film bicrystals with a symmetric [001] tilt of 24° . For

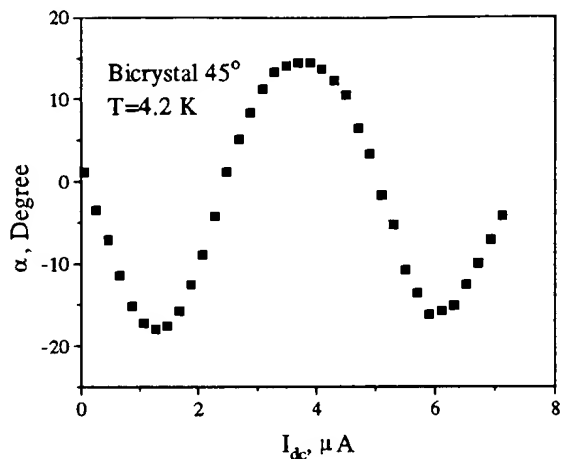


FIG. 2. Phase angle α between the driving current and the output voltage measured at 4.2 K as a function of the dc current I_{dc} , for an $\text{YBa}_2\text{Cu}_3\text{O}_{7-x}$ single junction interferometer circuit containing a symmetric 45° [001]-tilt grain boundary.

all of those samples nominally sinusoidal current-phase relations were observed, and all deviations of the apparent CPR from a sinusoidal one can be attributed to thermal noise [12,13].

The measured deviations from a sinusoidal dependence for the current-phase relations of these 45° bicrystals are startling. It is important to note that the effective Josephson penetration depth $\Lambda_J = [\Phi_0/(4\pi\mu_0\langle j_c \rangle \lambda)]^{1/2} \approx 5 \mu\text{m}$ is larger than the width of the junction b (narrow-junction limit). Here λ is the London penetration depth. Although several mechanisms are known to cause nonsinusoidal current-phase relations for narrow junctions fabricated from conventional superconductors, all of these mechanisms fail to account for the anomalous dependencies presented.

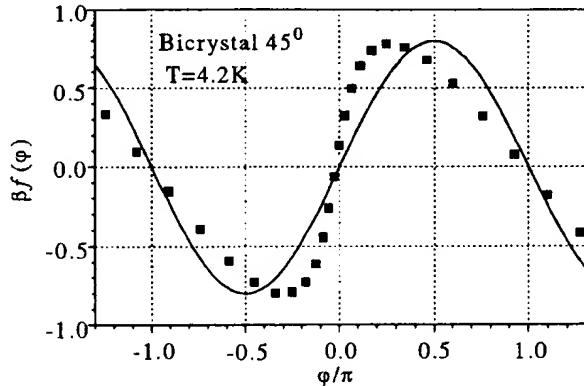


FIG. 3. The normalized current through the junction $\beta f(\varphi)$ as a function of the phase difference φ restored from the measured $\alpha(I_{dc})$ as shown in Fig. 2. For comparison, the function $\beta \sin(\varphi)$ with $\beta = 0.8$ is plotted as a solid line.

First, one potential source of such deviations is thermal noise. To evaluate its influence we consider a sinusoidal CPR and calculate with Eq. (3) the $\alpha(\varphi_{dc})$ dependence, assuming a thermally induced Gaussian spread $\rho(\varphi_n)$. With this, the value of $\tan \alpha(\varphi_{dc})$ is given by [12]

$$\tan \alpha(\varphi_{dc}) = k^2 Q \beta \int_{-\infty}^{\infty} \frac{\cos \varphi(\varphi_e, \varphi_n)}{1 + \beta \cos \varphi(\varphi_e, \varphi_n)} \rho(\varphi_n) d\varphi_n. \quad (4)$$

Using Eq. (4), minor deviations of the CPR from a standard sinusoidal behavior are well described quantitatively for 24° boundaries measured at 77 K [12]. However, no realistic set of β and φ_n exists to account for the large deviations of the CPR observed for the 45° boundaries.

Second, for weak links with a high current density, current-induced suppression of the order parameter in the electrodes close to the weak link can give rise to nonharmonic current-phase relations [16]. It is unrealistic that this effect is the cause for the deviations presented here, as the intragrain critical current density exceeds 10^7 A/cm^2 at 4.2 K and is therefore much larger than the grain boundary $\langle j_c \rangle < 4000 \text{ A/cm}^2$ at the same temperature.

Third, several additional mechanisms, described in [2], lead to deviations from a harmonic CPR. In all these cases, the slope of $f(\varphi)$ at $\varphi = 0$ is smaller than at $\varphi = \pi$, which is in contrast to our results. Therefore, these mechanisms cannot explain the current-phase relations observed either.

On the other hand, as will be pointed out in the following, the measured CPR can be accounted for by the unconventional order parameter symmetry of $\text{YBa}_2\text{Cu}_3\text{O}_{7-x}$ and by the microstructural properties of the grain boundaries, in particular by their faceted nature [17,18]. Interestingly, due to the $d_{x^2-y^2}$ -wave character of the order parameter, the faceting has a more significant influence on the electronic properties of boundaries with a misorientation close to 45° than on boundaries with considerably smaller misorientation angles [18]. This also concerns the CPR, as the 45° boundaries contain a higher density of facets that themselves show anomalous behavior. Two kinds of such anomalies, to be considered here, are described in the literature.

First, due to the sign difference of the adjacent lobes of the $d_{x^2-y^2}$ -wave order parameter, many facets are biased with an additional π phase shift (π facets) [17–19]. These phase shifts give rise to unconventional junction properties, such as a spontaneous generation of magnetic flux in the grain boundary junction [19–21]. As described in Ref. [21], the local phase difference $\varphi(x)$ along the grain boundary ($0 < x < b$) can be written as

$$\varphi(x) = \xi(x) + \psi(x), \quad (5)$$

where $\xi(x)$ is a rapidly alternating function accounting for the π phase shifts and for the spontaneously generated

magnetic flux in the junction, and $\psi(x)$ is the remaining slowly varying phase difference reflecting the magnetic flux in the interferometer loop. For a narrow junction ($b < \Lambda_J$), ψ is independent of x . With Eq. (5), the time-independent sine-Gordon equation, describing the spatial dependence of the local phase difference over the junction, becomes

$$\Lambda_J^2 \frac{\partial^2 \xi(x)}{\partial x^2} = \frac{j_c(x)}{\langle j_c \rangle} \sin[\psi + \xi(x)]. \quad (6)$$

The solution $\xi(x)$ of this equation, and thus the pattern of self-generated flux, depends on ψ . The redistribution of this flux by a change of ψ is expected to lead to remarkable deviations from a harmonic dependence for the CPR measured for the entire junction, also if the local CPR is nominally sinusoidal.

Second, it has been proposed [7,8] that the CPR of facets formed by the (110) and by the (100) planes of the adjacent grains is periodic with π and thus has a double periodicity as compared to the standard case. Transmission electron microscopy has revealed that 45° [001] tilt grain boundaries in $\text{YBa}_2\text{Cu}_3\text{O}_{7-x}$ tend to be composed for a considerable part of such facets [22]. For the whole junction, this leads to an anomalous CPR:

$$I = I_{c1} \sin \psi + I_{c2} \sin 2\psi, \quad (7)$$

by which the observed CPR can be described.

In summary, the current-phase relations of grain boundary junctions with a misorientation of 45° were measured with a modified Rifkin-Deaver method. The CPRs were deduced from measurements of the phase angle between the rf drive current and the rf tank voltage. The current-phase relations of the Josephson junctions showed pronounced deviations from a harmonic behavior, which cannot be accounted for by thermal noise or by other standard mechanisms, but are attributed to the $d_{x^2-y^2}$ -wave symmetry of the order parameter and the faceting of the grain boundaries.

We are grateful to A. Golubov and M. Kupriyanov for fruitful discussions. Part of this work has been performed at the IBM Zürich Research Laboratory. Financial support by the DFG (Ho 461/1-1) and the BMBF (13N6519 and 13N6918/1) is gratefully acknowledged. One of us

(H. H.) thanks the Royal Dutch Academy of Sciences and the University of Twente for their support.

- [1] B. D. Josephson, Phys. Lett. **1**, 251 (1962); Rev. Mod. Phys. **36**, 216 (1964).
- [2] K. K. Likharev, Rev. Mod. Phys. **51**, 101 (1979).
- [3] C. C. Tsuei, J. R. Kirtley, C. C. Chi, Lock See Yu-Jahnes, A. Gupta, T. Shaw, J. Z. Sun, and M. B. Ketchen, Phys. Rev. Lett. **73**, 593 (1994).
- [4] D. J. Van Harlingen, Rev. Mod. Phys. **67**, 515 (1995).
- [5] D. J. Scalapino, Phys. Rep. **250**, 329 (1995).
- [6] Yu. S. Barash, A. V. Galaktionov, and A. D. Zaikin, Phys. Rev. B **52**, 665 (1995).
- [7] W. Zhang, Phys. Rev. B **52**, 3772 (1995).
- [8] Y. Tanaka and S. Kashiwaya, Phys. Rev. B **53**, R11957 (1996).
- [9] H. Burkhardt (to be published).
- [10] S. S. Tinchev, Physica (Amsterdam) **222C**, 173 (1994).
- [11] V. Polushkin, S. Uchaikin, S. Knappe, H. Koch, B. David, and D. Grundler, IEEE Trans. Appl. Supercond. **5**, 2790 (1995).
- [12] V. Zakosarenko, E. V. Il'ichev, R. P. J. IJsselsteijn, and V. Schultze, IEEE Trans. Appl. Supercond. **7**, 1057 (1997).
- [13] E. V. Il'ichev, V. Zakosarenko, V. Schultze, H.-G. Meyer, H. E. Hoenig, V. N. Glyantsev, and A. Golubov, Appl. Phys. Lett. **72**, 731 (1998).
- [14] R. Rifkin and B. S. Deaver, Phys. Rev. B **13**, 3894 (1976).
- [15] D. Dimos, P. Chaudhari, J. Mannhart, and F. K. LeGoues, Phys. Rev. Lett. **61**, 219 (1988).
- [16] M. Yu. Kupriyanov, Pis'ma Zh. Eksp. Teor. Fiz. **56**, 414 (1992) [JETP Lett. **56**, 399 (1992)].
- [17] C. A. Copetti, F. Rüders, B. Oelze, Ch. Buchal, B. Kabius, and J. W. Seo, Physica (Amsterdam) **253C**, 63 (1995).
- [18] H. Hilgenkamp, J. Mannhart, and B. Mayer, Phys. Rev. B **53**, 14586 (1996).
- [19] J. Mannhart, H. Hilgenkamp, B. Mayer, Ch. Gerber, J. R. Kirtley, K. A. Moler, and M. Sigrist, Phys. Rev. Lett. **77**, 2782 (1996).
- [20] R. G. Mints and V. G. Kogan, Phys. Rev. B **55**, R8681 (1997).
- [21] R. G. Mints (to be published).
- [22] J. A. Alarco, E. Olsson, Z. G. Ivanov, P. A. Nilsson, D. Winkler, E. A. Stepanov, and A. Ya. Tzalenchuk, Ultramicroscopy **51**, 239 (1993).

EXHIBIT C

Lindström *et al.*, 2003, Physical Review Letters 90, 117002

Dynamical effects of an unconventional current-phase relation in YBCO dc-SQUIDS

T. Lindström,^{1,*} S.A. Charlebois,¹ A.Ya. Tzalenchuk,² Z. Ivanov,¹ M.H.S. Amin,³ and A.M. Zagoskin^{3,4}

¹*Department of Microelectronics and Nanoscience,
Chalmers University of Technology and Göteborg University, SE-412 96 Göteborg, Sweden*

²*National Physical Laboratory, Teddington, Middlesex, TW11 0LW, UK*

³*D Wave Systems Inc., 320-1985 Broadway, Vancouver, B.C., V6J 4Y3, Canada*

⁴*Physics and Astronomy Dept., The University of British Columbia,
6224 Agricultural Rd., Vancouver, V6T 1Z1 Canada*

(Dated: March 8, 2003)

The predominant *d*-wave pairing symmetry in high temperature superconductors allows for a variety of current-phase relations in Josephson junctions, which is to a certain degree fabrication controlled. In this letter we report on direct experimental observations of the effects of a non-sinusoidal current-phase dependence in YBCO dc-SQUIDS, which agree with the theoretical description of the system.

Keywords: Josephson Effect, High-Temperature Superconductivity, *d*-wave symmetry

It is well established [1] that the wave function of a Cooper pair in most cuprate high-temperature superconductors (HTS) has a *d*-wave symmetry. Its qualitative distinction from e.g. the anisotropic *s*-wave case is that the order parameter changes sign in certain directions, which can be interpreted as an *intrinsic* difference in the superconducting phase between the lobes equal to π .

The latter leads to a plethora of effects, like formation of Andreev bound states at surfaces and interfaces in certain crystallographic orientations [2, 3, 4]. The current-phase dependence $I_S(\phi)$ in Josephson junctions formed by *dd*-junctions, as well as by *sd*-junctions comprised of a cuprate and a conventional superconductor, depends both on the spatial orientation of the *d*-wave order parameter with respect to the interface, and on the quality of the latter [5, 6, 7, 8, 9]. Time-reversal symmetry can also be spontaneously violated and thus spontaneous currents generated [10, 11, 12]. Another effect can be doubling of the Josephson frequency [6, 13, 14].

In this letter we report on experimental observations of strong effects of an unconventional current-phase relation on the dynamics of two *dd*-junctions integrated into a superconducting interference device (SQUID) configuration.

Since $I_S(\phi)$ must be a 2π -periodic odd function, it can be expanded in a Fourier series. In the most cases only the first two harmonics give a significant contribution to the current:

$$I_S(\phi) = I_c^I \sin \phi + I_c^{II} \sin 2\phi \quad (1)$$

In Josephson systems of conventional superconductors the second harmonic will usually be negligible [15] but in *dd*-junctions the second harmonic may dominate. If $I_c^{II} > I_c^I/2$ the equilibrium state is no longer $\phi = 0$ but becomes double degenerate at $\phi = \pm \arccos(I_c^I/2I_c^{II}) \rightarrow \pm \pi/2$. The system can then spontaneously break time reversal symmetry by choosing either state. Spontaneous currents as well as fluxes can be generated in this state.

The potential will have the shape of a double well and there are reasons to believe that it will be possible to observe quantum-coherence in this system. The presence of a 2nd harmonic in the current-phase relation(CPR) of a *dd*-junction was confirmed by Il'ichev et al [8].

A non-sinusoidal CPR of the junctions will change the dynamics of a dc-SQUID [16]. Regarding the junctions as magnetically small, the supercurrent through the SQUID in the presence of an external flux $\Phi_x \equiv \Phi_0 \cdot (\phi_x/2\pi)$ can be written as

$$I_s(\phi, \phi_x) = I_c^I \sin \phi + I_c^{II} \sin(2\phi) + I_c^I \sin(\phi + \phi_x) - I_c^{II} \sin 2(\phi + \phi_x) \quad (2)$$

The critical current through the SQUID is given by the usual expression $I_c(\phi_x) = \max_\phi I_s(\phi, \phi_x)$. The time-averaged voltage over the SQUID in the resistive regime is readily obtained in the resistively shunted junction (RSJ) approximation. By introducing $\delta[\phi, \phi_x] = \phi_2 - \phi_1$ and applying the same method as in [17] with the necessary generalizations, we obtain for the average voltage over the SQUID

$$V^{-1} = \frac{G_1 + G_2}{2\pi} \int_{-\pi}^{\pi} d\phi \left[I - (G_1 + G_2) \frac{h}{2e} \frac{d\delta}{dt} - I_1 \left(\phi + \frac{\delta}{2} \right) - I_2 \left(\phi - \frac{\delta}{2} \right) \right]^{-1}. \quad (3)$$

Here $G_{1,2}$ are the normal conductances of the junctions, and

$$\delta + \phi_x + \frac{\pi L}{\Phi_0} (I_2(\phi - \delta/2) - I_1(\phi + \delta/2)) = 0, \quad (4)$$

gives the difference, δ , in phase drops across each junction. In deriving (3,4) we have assumed that the inductance L is equally divided between the SQUID arms. We have also neglected the spontaneous magnetic fluxes in the *dd*-junctions, due to their small amplitude [11, 18].

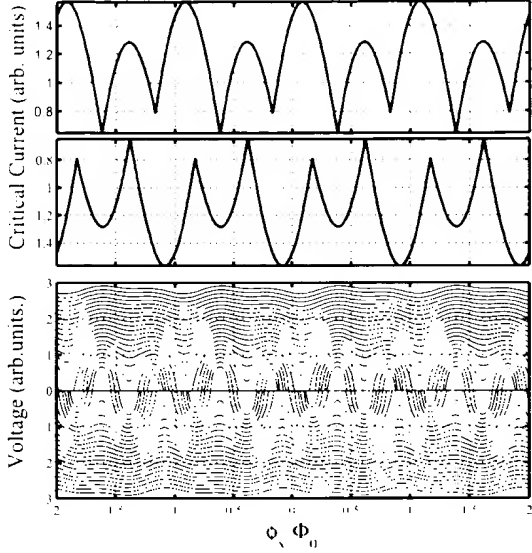


FIG. 1: The results of simulations of the $I_c - \phi_r$ and $V - \phi_r$ dependence for a dc-SQUID with $I_{c1}^I = 1$, $I_{c2}^I = 0.1$, $I_{c1}^{II} = 0.2$ and $I_{c2}^{II} = 0.1$ (arb. units). The different curves correspond to bias currents in the range $I = I_{c1}^I$ to $I = 5I_{c1}^I$. We assume $L = 0$ and $G_1 = G_2$.

Though (4) is only explicitly solvable in the limit $L \rightarrow 0$, it always yields $\delta[-\phi_r, -\phi_r] = -\delta[\phi_r, \phi_r]$. This means that the usual inversion symmetry is retained.

The results of numerical calculations based on (2) and (3) are shown in fig 1. The cusps in the critical current correspond to the points at which the global maximum in (1) switches from one local maximum to another [16]. Note the quasi- $\Phi_0/2$ -periodicity of the current isolines in the $V - \phi_r$ picture, reflecting the current-phase dependence (1), and their shift along the Φ_r -axis, which depends on the sign of the bias current (as it must to maintain the central symmetry with respect to the origin). The shift does not depend on the magnitude of the current since we neglect the self-inductance. For large biases the Φ_0 -periodicity is restored. Indeed, as the bias grows, one set of minima of the washboard potential, $U = (h/2e)[-I^I \cos \phi + (I^{II}/2) \cos 2\phi - I_{c2}^I]$, disappears first unless the first harmonic I^I is *exactly* zero.

We have fabricated and studied a large number of dc-SQUIDs. The samples were fabricated from 250 nm thick YBCO-films deposited on SrTiO_3 -bicrystals. The grain-boundary junctions (GBJs) are of the asymmetric [001]-tilt type with the misorientation angle of 45° ($0^\circ - 45^\circ$ GBJ). For more information on GBJs see for example reference [19].

The pattern was defined using E-Beam lithography and then transferred to a carbon mask employing a multi-step process. Finally, the YBCO is etched through the mask using ion-milling. This scheme allows us to fabricate high-quality bicrystal junctions as narrow as 0.2 μm ,

as has been reported elsewhere [20]. In the SQUIDs under investigation the junctions are nominally 2 μm wide; hence the fabrication-induced damage of the junctions is small.

The measurements were done in an EMC-protected environment using a magnetically shielded LHe-cryostat. However, the magnetic shielding is imperfect, as is evident from the fact, that the expected zero-field response of our SQUIDs is not exactly at zero. The measuring electronics is carefully filtered and battery-powered whenever possible. In order to measure the dependence of the critical current on the applied field we used a voltage discriminator combined with a sample-and-hold circuit. All measurements reported here were performed at 4.2K.

The SQUID loops are $15 \times 15 \mu\text{m}^2$. The numerically calculated inductance [21] is approximately 25 pH, yielding the factor $\beta = 2\pi L I_c / \Phi_0$ between 0.5-2.

The SQUIDs were largely non-hysteretic with a resistance of about 2 Ω . The measured critical current varies from sample to sample but is in the range of tens of microamperes giving a current density of the order of $J_c = 10^3 \text{ A/cm}^2$. The estimated Josephson penetration length $\lambda_J = \Phi_0 / \sqrt{4\pi\mu_0 j_c \lambda_L}$ is approximately 2 μm in all junctions, which means that the junctions are magnetically short. This is supported by the quasi-period of the pattern in fig 2 being close to the expected value $\phi_0/2\lambda_L w$ [17]. The differential conductance curves do not show any trace of a zero bias anomaly (ZBA), as is expected for $0^\circ - 45^\circ$ GBJs. ZBAs has been observed by other groups in GBJs with other orientations [2].

The critical current is plotted as a function of applied magnetic field for two SQUIDs in fig.3. The result is in qualitative agreement with theory if we assume that the SQUID junctions have different ratios of the 1st and 2nd harmonics of the critical current. This assumption is supported by the fairly small modulation depth (it is easy to see from equation (2) that I_c would go exactly to zero in a SQUID with junctions of identical I_{c2}/I_{c1}).

We can fit the data to equation (2), if we compensate for the residual background magnetic field and assume that we have a small excess current (of the order of a few μA) in the junctions. The fitting parameters again confirm that there is a large asymmetry between the arms of the SQUIDs. Note, that the model does not consider the flux penetration into the junctions.

The result for fields of the order of mT is presented in fig.2 which shows the I_c -modulation of the SQUID enveloped by an anomalous Fraunhofer-pattern quite similar to what has been reported by other groups [22, 23] for $0^\circ - 45^\circ$ GBJs. Note the inversion symmetry of the pattern with respect to the origin. That the global maximum is not in the center can be explained in several ways; it has been shown for example that this could be due to the presence of so-called π -loops in the junction interface [24].

Figure 4 shows the $V - B$ -dependence of one of the

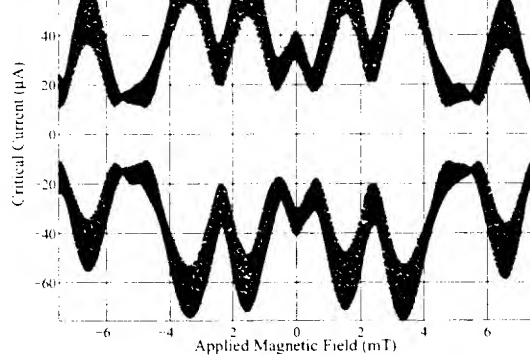


FIG. 2: Critical current as a function of magnetic field at 4.2K. The dashed box indicates the area plotted in fig. 3a.

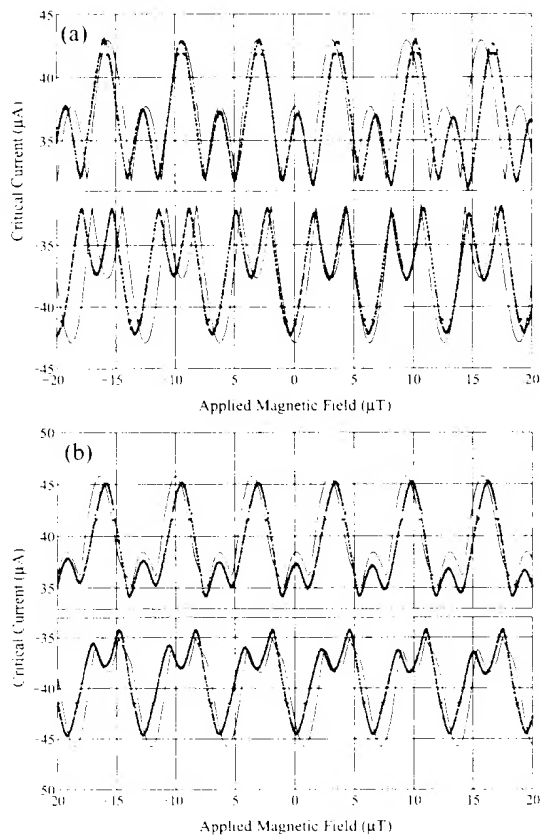


FIG. 3: Critical current as a function of applied magnetic field for two different SQUIDs that are nominally identical. The solid line represents the fitted expression. The fitting parameters are as follows: (a) $I_{c1}^I = 9 \mu\text{A}$, $I_{c2}^I = 0.3 \mu\text{A}$, $I_{c1}^{II} = 3.7 \mu\text{A}$ and $I_{c2}^{II} = 22.7 \mu\text{A}$ (b) $I_{c1}^I = 7.8 \mu\text{A}$, $I_{c2}^I = 3.0 \mu\text{A}$, $I_{c1}^{II} = 5.3 \mu\text{A}$ and $I_{c2}^{II} = 4.3 \mu\text{A}$. In both cases the fit has been adjusted with respect to the residual background field and the excess current of the junctions.

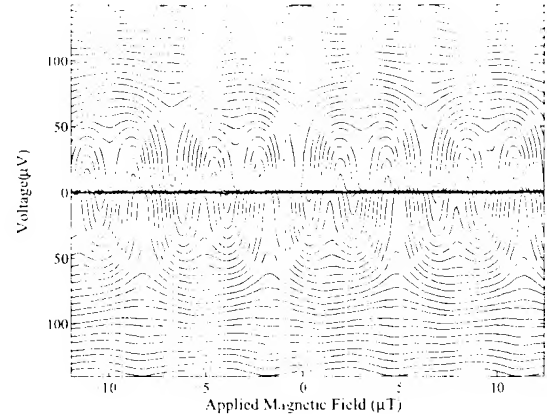


FIG. 4: Voltage modulation as a function of applied magnetic field for the SQUID whose $I_c - B$ is shown in fig. 3a. The pattern is again inversion symmetric. Note the sign change at $100 \mu\text{V}$ which we believe is due to a LC-resonance in the SQUID loop.

SQUIDs. The pattern is again field inversion-symmetric. The overall structure is the same as in the model dependence of fig.1, but there is also an additional shift due to self-field effects, which depends on the magnitude of the bias current and corresponds (at maximum) to a flux $\sim 0.1\Phi_0$. In a beautiful experiment a similar dependence was recently observed by Baselmans et al in a Nb-Ag-Nb SNS junction where current-injectors were used to change the occupation of current-carrying states in the normal region [25]. A deviation from the model occurs at $V=100 \mu\text{V}$ where the minima and maxima switch. This is probably due to an LC-resonance in the SQUID. Taking $L = 25 \text{ pH}$, this would require $C = 0.8 \text{ pF}$, which agrees with our measurements on single junctions

Remarkably, the observed offset of the $V - B$ -characteristics with respect to the *direction* of the bias current appears to be a much more robust manifestation of the presence of a second harmonic of the Josephson current, than the shape of the $I_c - B$ curves itself. We observed the shift even in SQUIDs with the smallest junctions down to $0.5 \mu\text{m}$ wide, where the deviations from the usual sinusoidal CPR were not obvious from the $I_c - B$ dependence.

Generally the nature of the transport through a GBJ will depend on its transmissivity D . Illichev et al. [8] have reported values of D as high as 0.3 in symmetric ($22.5^\circ - 22.5^\circ$) *dd* junctions as opposed to the usual estimate for a GBJ, $D \sim 10^{-5} - 10^{-2}$. Since usually $I_c^{II}/I_c^I \propto D$, a high-transmissivity GBJ is required in order to observe effects of the second harmonic. An estimate of the *average* transmissivity of our junctions would be $\rho_{ab}l/R_N A \sim 10^{-2}$ [26] assuming l , the mean free path, to be equal to 10 nm and a resistivity in the a-b plane ρ_{ab} equal to $10^{-4} \Omega\text{cm}$. This is still too low to explain the strong 2nd harmonic we observe. However, it is known

from, e.g., TEM-studies [19], that the grain-boundary is far from uniform: the properties can significantly vary depending on the local properties of the interface, effects such as oxygen diffusion out of the GB etc., which are difficult to control. It is therefore reasonable to assume that there are many parallel transport channels through the GB[27, 28]. Channels with high transmissivity dominate the transport and might have $D \sim 0.1$ even though the *average* transmissivity is much lower. This is also consistent with the fact that most of our SQUIDs seem to be highly asymmetrical which is to be expected if the distribution of channels is random. The ratios of I_c^I and I_c^{II} can vary as much as ten times between two junctions in the same SQUID, even though the fluctuations of the *total* I_c from sample to sample are much smaller. It is also clear from general considerations that a high value of I_c^{II} excludes a high value of I_c^I , since the 2nd harmonic usually dominates if the odd harmonics of the supercurrent are cancelled by symmetry [29].

Recent studies of 0° – 45° GBJs have demonstrated that the SQUID-dynamics can be altered by the d-wave order parameter in YBCO [30]. It is however important to point out that our results *do not* directly relate to e.g. tetracryystal π -SQUID experiments: the latter crucially depend on having one π -junction with negative critical current, but still only the first harmonic present in $I_c(\phi)$. Our SQUIDs have a conventional geometry, but unconventional current-phase relations.

One explanation for the pronounced effects of the 2nd harmonic could be that relatively large sections of the interface are highly transparent and have a low degree of disorder. This in turn could be related to our fabrication scheme which seems to preserve the integrity of the barrier. This makes feasible their applicability in the quantum regime and supports our expectations that quantum coherence can be observed in this kind of structures.

To summarize, we have observed very pronounced 2nd harmonic in the current-phase relation of a 'conventional' YBCO dc-SQUID with 0° – 45° grain boundary junctions. It has strongly influenced the SQUID dynamics. All details of the SQUID behavior were explained within a simple model of a dd-junction with relatively high transparency. We believe that these effects are important for better understanding of HTS Josephson junction and SQUIDs.

Discussions with Evgenii Il'ichev, Alexander Golubov, Tord Claeson, and John Gallop are gratefully acknowledged. The work is in part supported by The Board for Strategic Research (SSF) via the "OXIDE" program, the Science Research Council, and the "Fonds quibcois de la recherche sur la nature et les technologies". The processing work is done at the MC2 process lab at Chalmers University of Technology

- [1] C. Tsuei and J. Kirtley, *Reviews of Modern Physics* **72**, 969 (2000).
- [2] L. Alff et al., *Physical Review B* **58**, 11197 (1998).
- [3] T. Löfwander, V. Shumeiko, and G. Wendin, *Superconductor Science & Technology* **14**, R53 (2001).
- [4] C.-R. Hu, *Physical Review Letters* **72**, 1526 (1994).
- [5] S. Yip, *Physical Review B* **52**, 3087 (1994).
- [6] A. Zagoskin, *Journal of Physics: Condensed Matter* **9**, L419 (1997).
- [7] E. Il'ichev et al., *Physical Review B* **60**, 3096 (1999).
- [8] E. Il'ichev et al., *Physical Review Letters* **86**, 5369 (2001).
- [9] P. Komissinski et al., *Europhysics Letters* **57**, 585 (2002).
- [10] A. Huck, A. van Otterlo, and M. Sigrist, *Physical Review B* **56**, 14163 (1997).
- [11] M. Amin, A. Omelyanchouk, and A. Zagoskin, *Physical Review B* **63**, 212502 (2001).
- [12] S. Östlund, *Phys. Rev. B* **58**, R14757 (1998).
- [13] T. Löfwander, G. Johansson, M. Hurd, and G. Wendin, *Physical Review B* **57**, R3225 (1998).
- [14] H. Arie et al., *Physical Review B* **62**, 11864 (2000).
- [15] M. Keene, C. Gough, and A. Rae, *Journal of Physics: Condensed Matter* **3**, 6079 (1991).
- [16] M. H. S. Amin, M. Coury, and R. Rose, *IEEE Trans. Appl. Supercond.* **12**, 1877 (2002).
- [17] A. Barone and G. Paterno, *Physics and Applications of the Josephson Effect* (John Wiley & Sons, 1982).
- [18] M. Amin, S. Rashkeev, M. Coury, A. Omelyanchouk, and A. Zagoskin, *Physical Review B* **66**, 174515 (2002).
- [19] H. Hilgenkamp and J. Mannhart, *Reviews of Modern Physics* **74**, 297 (2002).
- [20] A. Tzalenchuk et al., *Applied Physics Letters* *Submitted* (2002).
- [21] M. Khapaev, A. Kidiyarova-Shevchenko, P. Magnelind, and M. Kupriyanov, *IEEE Transactions on Applied Superconductivity* **11**, 1090 (2001).
- [22] J. Mannhart, B. Mayer, and H. Hilgenkamp, *Zeitschrift für Physik B (Condensed Matter)* **101**, 175 (1996).
- [23] W. Neils and D. van Harlingen, *Physica B* **284-288**, 587 (2000).
- [24] H. Smilde et al., *Physical Review Letters* **88**, 057004 (2002).
- [25] J. Baselmans, T. Heikkil, B. van Wees, and T. Klapwijk, *Phys. Rev. Lett.* **89**, 207002 (2002), the pronounced 2nd harmonic in this experiment appears due to non-equilibrium effects, see e.g. J.C. Clarke "Charge Imbalance" in K.E. Gray (ed.) *Nonequilibrium Superconductivity, Phonons and Kapitza Boundaries*, NATO ASI Series, Plenum, NY(1981), p. 353.
- [26] G. Blonder, M. Tinkham, and T. Klapwijk, *Physical Review B* **25**, 4515 (1982).
- [27] Y. Naveh, D. Averin, and K. Likharev, *Physical Review Letters* **79**, 3482 (1997).
- [28] E. Sarnelli, G. Testa, and E. Esposito, *Journal of Superconductivity* **7**, 387 (1994).
- [29] Y. Barash, *Physical Review B* **61**, 678 (2000).
- [30] B. Chesca et al., *Physical Review Letters* **88**, 177003 (2002).